ISSN 2229-5518

Study of Forced Convection Heat Transfer with non-Newtonian Fluid in circular tube

Ahmed Hammodi Ali , Hassanian Ghani Hameed and Hussein Awad Kurdi Saad

Abstract— In this investigation, study of heat transfer forced convection in two dimensional of non-Newtonian flow inside a circular tube under constant heat flux with laminar flow has been analyzed numerically. Wide ranges of Reynolds number (220, 755, 1315 and 1875), prandtl number (1.67 , 4.67 and 13.67) and power law model "Prandtl – Eyring.(P.E)" (0.1,0.5,1 and 5) are adopted. To explain the behavior of temperature field and flowing fluid, the vortices, stream functions in addition to temperature distribution formulas are used. Besides that, the relations between average Nusselt number, Reynolds number, Prandtl number and power law model are presented. The results demonstrated that increase in both Reynold number and Prandtl's number have a positive effect on heat transfer enhancement for the model of Prandtl - Eyring for non-Newtonian fluid. Also, increasing of Prandtl - Eyring lead to increasing of Heat transfer coefficient for a given rest parameters and an essential reduction in time elapsed for steady state was showed..

Index Terms— Forced conection, non-Newtonian, Power law model, Constant heat flux.

1 Introduction

Forced convection is one of the most important modes of heat transfer. Forced convection, which takes place by an external driving force forcing the fluid to flow on the tube, and generally, the rate of heat transfer, depends upon the Reynolds number and Prandtl number. Also, non-Newtonian fluid (Pr>1)take up wide range of applications such as multi-grade oils, paints, , liquid detergents printing inks and industrial highly viscous liquids such as automotive oils and etc. Therefore, several studies studied the heat transfer coefficient when Non-Newtonian fluid instead of Newtonian one. H. S. Yogosh Showed extension of Graetz-Nusselt theory of heat transfer to non-Newtonian flow. He used ordinary partial differential equation in addition to power law model for non-Newtonian flow profile. The results showed that degrees power law model has a clear effect on temperature distribution and increasing of Nusselt number. [1].Chhabra et al. Investigated incompressible, steady state and non-Newtonian fluid for power law model past circular tube numerically. Different values of Re (1, 20 and 40), power law indices “n” (0.2 - 1.4) and blockage ratios (0.037, 0.082 and 0.164) were used. The results showed increase of blockage ratios or decrease in index of power law has the same effect on velocity profile. [2]. Nagendra et al. were investigated the combination effect of magneto-hydrodynamic heat, momentum and mass (species) transfer theoretically on external boundary layer of a horizontal circular cylinder. Both of thermophoresis and Brownian motion effect on heat and convective conditions of nanoparticle mass transfer were studied. Results illustrated that a strong relationship among magnetic intensity, nanoparticles size with increasing of heat transfer rate. [3]. Soares et al. Were studied numerically the incompressible, steady across long cylinder with power law model. The behavior of different parameters investigated at low and high Reynolds number and the results were validating with those at literature. [4]. A flow of Non-Newtonian fluid in micro-channels and non-circular pipes are studied numerically by Muzychka et al. A simple power law model depended on Rabinowitsch–Mooney formulation was employed by using square root of cross- sectional area and scale of length as new characteristics. The results showed that wall shear stress in dimensionless form has a weak effect on shape of duct. [5]. A natural convection heat transfer with laminar flow in square cavity filled with copper–water nanofluid heated differentially was investigated numerically by Santra et al. Two parameters for an incompressible non-Newtonian fluid with model of power law were considered.[6]

Nomenclature

Symbols Variables

Symbol	Description	Units
B, C	Fluid consistency indices for Prandtl – Eyring model	———
C_f	Coefficient of Friction	———
d	Diameter of Tube	m
H	Heat Transfer Coefficient	$W/m^2.K$
K	Thermal Conductivity	W/m.K
L	Length of Tube	m
Nu_z	Local Nusselt Number	———
$\overline{Nu}$	Average Nusselt Number	———
P	Pressure	Pa
P.E	Fluid index of Prandtl – Eyring model	———
Pr	Prandtl number	———
q"	Heat Flux	W/m^2
r	Radial Coordinate	m
Re	Reynolds number	———
T	Temperature	K
u	Axial Velocity	m/s
v	Radial Velocity	m/s
z	Axial Coordinate	m

ISSN 2229-5518

Greek Symbols

Symbol	Description	Units
C_p	Heat capacity	KJ/Kg. K
μ	Dynamic viscosity	m^2/s
ρ	Density	Kg/m^3
τ	Stresses	Pa
ψ	Stream function	m^2/s
ω	Vorticity	1/s
∇	Laplacian operator	———

2 Mathematical Formulation

The schematic of physical model besides the system of coordinates are presented in Fig.(1). It's a circular horizontal tube. The descriptions of flow were laminar, non-Newtonian, incompressible flow with constant fluid properties

2.1 Goerning Equations

For non-Newtonian fluid in case of two-dimensional steady state with constant properties, the governing equations in their primitive form are[7] and [8]:

Continuity Equation

$$\frac{\partial u}{\partial z}+\frac{1}{r}\frac{\partial}{\partial r}(rv)=0 \qquad (1)$$

Momenteum Equation in z-direction

$$\rho\left(u\frac{\partial u}{\partial z}+v\frac{\partial u}{\partial r}\right)=-\frac{\partial p}{\partial z}+\frac{\partial \tau_{zz}}{\partial z}+\frac{\partial \tau_{zr}}{\partial r} \qquad (2)$$

Momenteum Equation in z-direction

$$\rho\left(u\frac{\partial v}{\partial z}+v\frac{\partial v}{\partial r}\right)=-\frac{\partial p}{\partial r}+\frac{\partial \tau_{rz}}{\partial z}+\frac{\partial \tau_{rr}}{\partial r} \qquad (3)$$

Energy Equation

$$\rho C_p\left(u\frac{\partial T}{\partial z}+v\frac{\partial T}{\partial r}\right)=k\left(\frac{\partial^2 T}{\partial z^2}+\frac{\partial^2 T}{\partial r^2}+\frac{1}{r}\frac{\partial T}{\partial r}\right) \qquad (4)$$

According to [9], the model of Prandtl - Eyring for non-Newtonian fluid can be expressed as:

$$\tau=B(\sinh)^{-1}\left(C\frac{\partial u}{\partial n}\right) \qquad (5)$$

Therefore, the shear stresses are

$$\tau_{zz}=2B\sinh^{-1}\left(C\frac{\partial u}{\partial z}\right) \qquad (6)$$

$$\tau_{rr}=2B\left[\sinh^{-1}\left(C\frac{\partial v}{\partial r}\right)+\frac{v}{r}\right] \qquad (7)$$

$$\tau_{zr}=\tau_{rz}=B\sinh^{-1}\left[C\left(\frac{\partial u}{\partial z}+\frac{\partial v}{\partial r}\right)\right] \qquad (8)$$

Where B and C are the coefficients of consistency of the model of Prandtl- Eyring. However, the stream function-vorticity equation has some attractive features. The pressure makes no appearance and instead of dealing with continuity, momentum and energy equations, it need solve only three equations to get temperature, vorticity and stream function.The stream functions and vorticity in polar coordinate are[10]and[11]:

$$u=\frac{\partial\psi}{\partial z}\ ,\ v=\frac{\partial\psi}{\partial r}\ \ and\ \ -\omega=\frac{\partial u}{\partial z}+\frac{\partial v}{\partial r}-\frac{v}{r} \qquad (9)$$

From the velocity component in terms of the stream function in addition to definition of the vorticity , and substituting the values of (τ) in equations (2) and (3) in momentum equations, then cross differentiating of equations (2) and (3) " equation (2) with respect to r-direction and (3) with respect to z-direction" then eliminate the pressure term. Therefore, a new group of equations with independent variable (ψ, ω) were appeared:

$$-\omega=\frac{\partial^2\psi}{\partial z^2}+\frac{\partial^2\psi}{\partial r^2}-\frac{1}{r}\frac{\partial\psi}{\partial r} \qquad (10)$$

$$\rho\left(\frac{\partial\psi}{\partial r}\frac{\partial\omega}{\partial z}+\frac{\partial\psi}{\partial z}\frac{\partial\omega}{\partial r}\right)=\mu\left\{\begin{array}{l} BC\left[\frac{\partial^2\omega}{\partial z^2}+\frac{\partial^2\omega}{\partial r^2}\right]+BC\left[\frac{1}{r}\frac{\partial\omega}{\partial r}\right] \\ +BC\left[\frac{\partial D_1}{\partial z}+\frac{\partial D_2}{\partial r}-\frac{\partial D_3}{\partial r}-2\frac{\partial D_4}{\partial r}\right] \\ +BCD_5 \end{array}\right\} \qquad (11)$$

$$\rho C_p\left(\frac{\partial\psi}{\partial r}\frac{\partial T}{\partial z}+\frac{\partial\psi}{\partial z}\frac{\partial T}{\partial r}\right)=k\left\{\frac{\partial^2\omega}{\partial z^2}+\frac{\partial^2\omega}{\partial r^2}+\frac{1}{r}\frac{\partial\omega}{\partial r}-\frac{\omega}{r^2}\right\} \qquad (12)$$

where:

Ahmed Hammodi Ali is a full time lecturer
at Engineering Technical College of Al -Najaf
Al-Furat Al-Awsat Technical University /Iraq
E-mail: *ahmead_new@yahoo.com*

$$D_1 = \frac{\dfrac{\partial^3\psi}{\partial z\partial r^2} - \dfrac{\partial^3\psi}{\partial z^3}}{\sqrt{1+\left[C\left(-\dfrac{\partial^2\psi}{\partial z^2}+\dfrac{\partial^2\psi}{\partial r^2}\right)\right]^2}} \tag{13}$$

$$D_2 = \frac{\dfrac{\partial^3\psi}{\partial z\partial r^2} - \dfrac{\partial^3\psi}{\partial z^3}}{\sqrt{1+\left[C\left(-\dfrac{\partial^2\psi}{\partial z^2}+\dfrac{\partial^2\psi}{\partial r^2}\right)\right]^2}} \tag{14}$$

$$D_3 = \frac{-\dfrac{\partial\psi}{\partial r}}{\sqrt{1+\left[C\left(\dfrac{\partial^2\psi}{\partial r^2}\right)\right]^2}} \tag{15}$$

$$D_4 = \frac{\dfrac{\partial^3\psi}{\partial z\partial r^2}}{\sqrt{1+\left[C\left(\dfrac{\partial^2\psi}{\partial r\partial z}\right)\right]^2}} \tag{16}$$

$$D_5 = \left[\begin{array}{l}\dfrac{\partial^4\psi}{\partial z^4}+\dfrac{\partial^4\psi}{\partial r^4}+2\dfrac{\partial^4\psi}{\partial z^2\partial r^2}+ \\ \dfrac{1}{r}\dfrac{\partial^2\psi}{\partial r^2}+\dfrac{\partial^2\psi}{\partial z^2}+\dfrac{\partial^2\psi}{\partial r^2}-\dfrac{1}{r}\dfrac{\partial\psi}{\partial r}\end{array}\right] \tag{17}$$

and

$\Pr = \dfrac{\nu}{\alpha}$ is Prandtl number (18)

$\mathrm{Re} = \dfrac{u\,d}{\nu}$ is Reynold number (19)

$\mathrm{P.E} = \dfrac{C\,\alpha}{L^2}$ is power law model (20)

And according to[11],the shear stress is defined as

$$\tau_w = \mu\left.\frac{\partial u}{\partial r}\right|_{r=r_o} \tag{21}$$

So, the coefficient of friction is

$$C_f = \frac{\tau_w}{\frac{1}{2}\rho u_{in}^2} \tag{22}$$

Also, the local and Average Nusselt number as [12] mention respectively is

$$Nu = \frac{qd}{k\Delta T} \tag{23}$$

$$\overline{Nu} = \frac{1}{L}\int_0^L Nu\,dz \tag{24}$$

2.2 Boundary Conditions

The boundary conditions used to solve the governing equations (10), (11) and (17) are

1. Inlet section

$u=u_{in}$

v=0

$T=T_{in}$

2. Outlet section

$$\frac{\partial u}{\partial z} = \frac{\partial r}{\partial z} = 0$$

3. wall surface

u=v=0

$$\frac{\partial T}{\partial r} = \frac{q}{k}$$

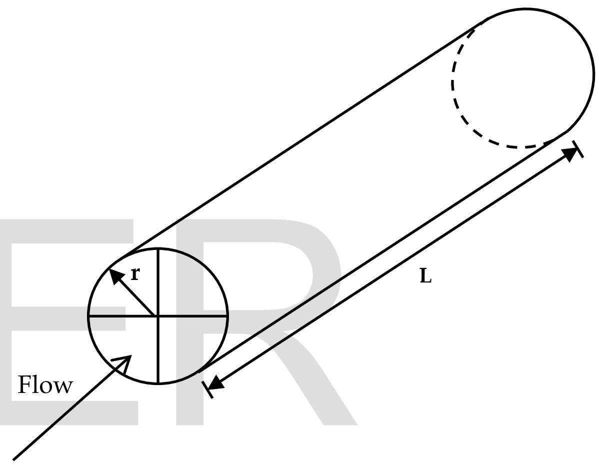

Fig.(1). The circular tube and the coordinates axis

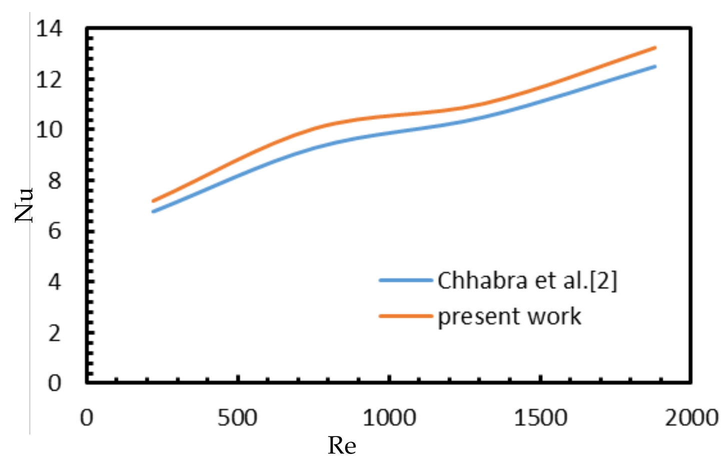

Fig.(2). Comparison of Nu no. between present work and Chhabra et al. [2]

4. Numerical Solution

The numerical method has been developed to deals with problems having complicated geometry involving different boundary conditions and non-linearity in complex equations. In this work, a computational technique for the solution of the vorticity, stream function and energy equations, were performed by using a finite volume method (FVM) to obtain the discretization form for these equations. These discretized equations were solved by using a SIMPLE algorithm with a hybrid scheme. A computer program based on this algorithm and using Fortran 90 language was built to meet the requirements of the problem. Besides that , the results were graphed by Tech-Plot program. The SIMPLE algorithm was based on the staggered grid in which the variables staggered midway between the grids intersections were used to obtain the numerical results.

4. Validation

To show the validation of numerical studies for fluid flowing inside circular tube. simulated results of Nusselt number versus Reynolds number are compared with that predicted by **Chhabra et al.** [2] at figure (2). Comparing the results at steady state conditions for different Reynolds number, a reasonably good agreement is exhibited between two sets of computational results.

5. Results and Dissection Discussion

The temperature distribution in the flow direction for constant heat flux and different values of power law model "Prandtl – Eyring (P.E) are presented in the figures (3) and (4). It's clear from these figures that if the P.E increase, the temperature distribution also enhanced. It's also showed that the layer of hottest flow is adjacent to wall of tube, then the temperature of flow layers decrease gradually towered to center. In addition to , the time elapsed for reaching to steady state condition at maximum value of (P.E) is less than of the rest of other cases. It's worth to mention, according to figure (4), increase in Reynolds number will accelerate and enhance of heat transfer rate between tube wall and particles of non-Newtonian fluid. The possible reason that the thermal entrance length is taller for the high Reynolds number than for the smaller one.

Figures (5) and (6) show arrangement of Nusselt number as a function of axial position with prandtl number for all values of Reynolds numbers and power law model. One of the most important factors effectual in definition of Nusselt number is mode of flow(Reynolds number) and type of flow (prandtl number). The local Nu began with a maximum value at the inlet section of tube. Then, the local Nu decrease with axial position along the flow direction because rapprochement between wall and fluid. Also, as the power law model increase, the local Nusselt number increase due to the changing of boundary layer thickness and high convective heat transfer.

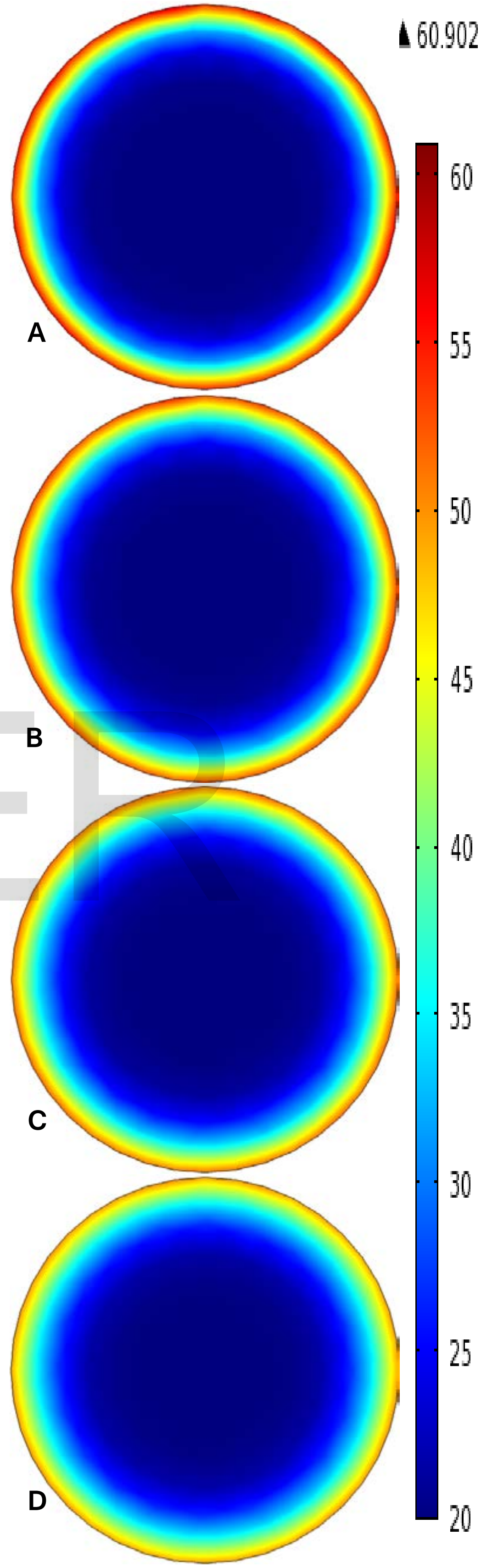

Fig.(3). Variation of Temp. disterbuion for Re=220 and Pr=4.67 where(A) P.E=0.1(B) P.E=0.5 (C) P.E=1 (D) P.E=5

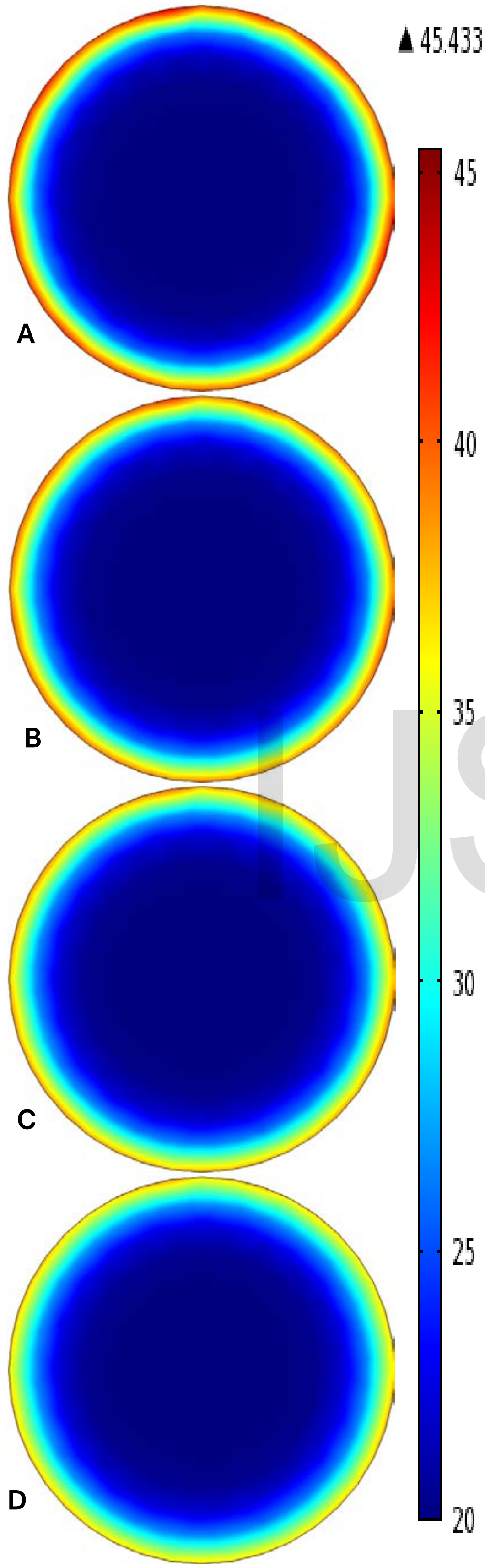

Fig.(4). Variation of Temp. disterbuion for Re=1315 and Pr=4.67 where(A) P.E=0.1(B) P.E=0.5 (C) P.E=1 (D) P.E=5

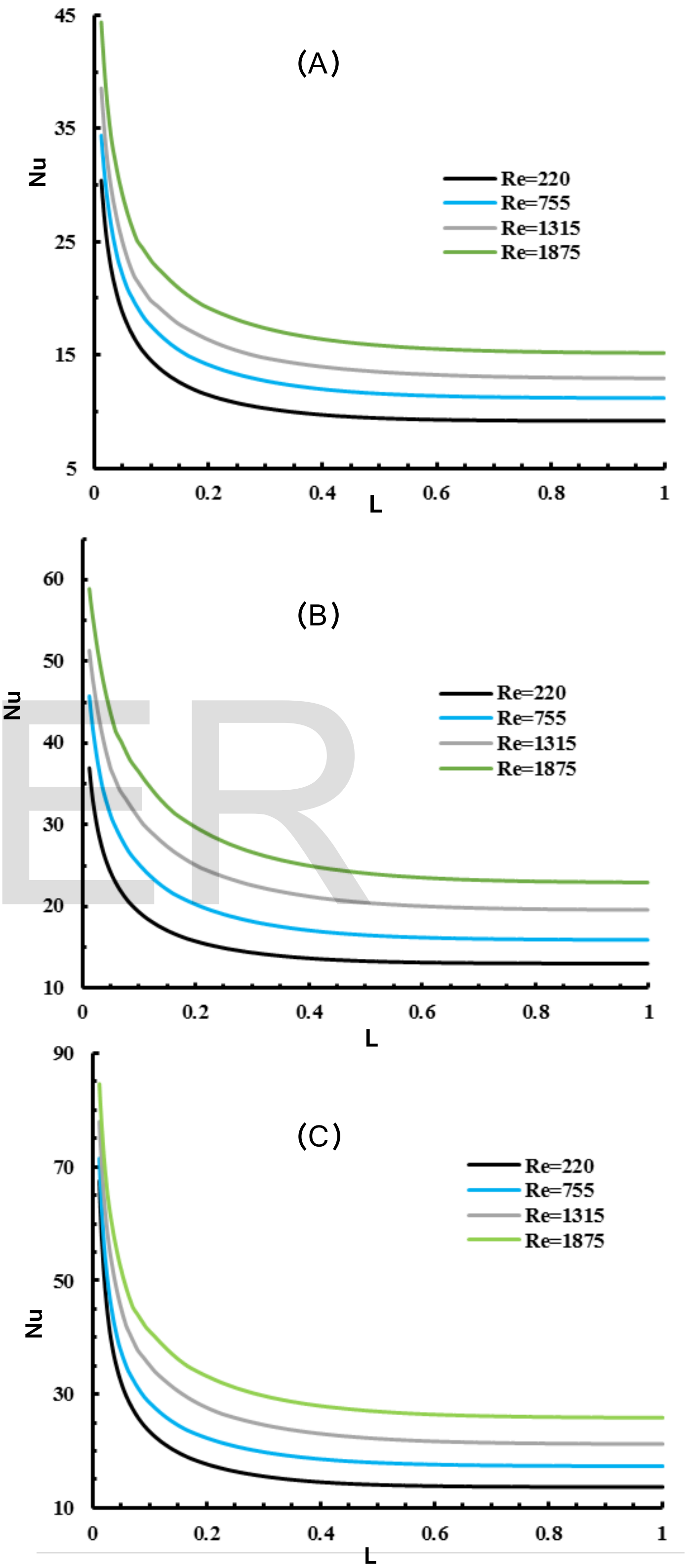

Fig.(5). Variation of (Nu) with of (L) at P.E=0.5 where (A) Pr=1.67 (B) Pr=4.67 (C) Pr=13.67

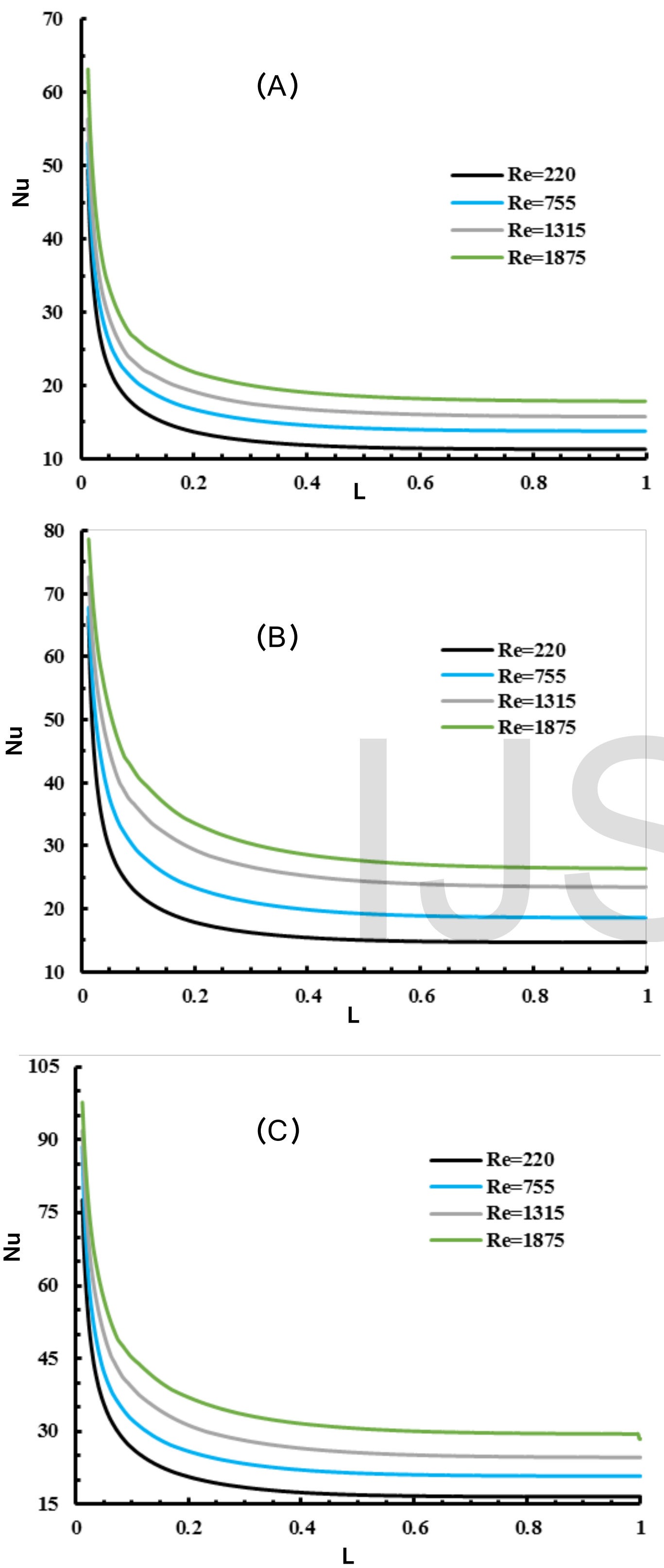

Fig.(6). Variation of (Nu) with of (L) at P.E=5 where (A) Pr=1.67 (B) Pr=4.67 (C) Pr=13.67

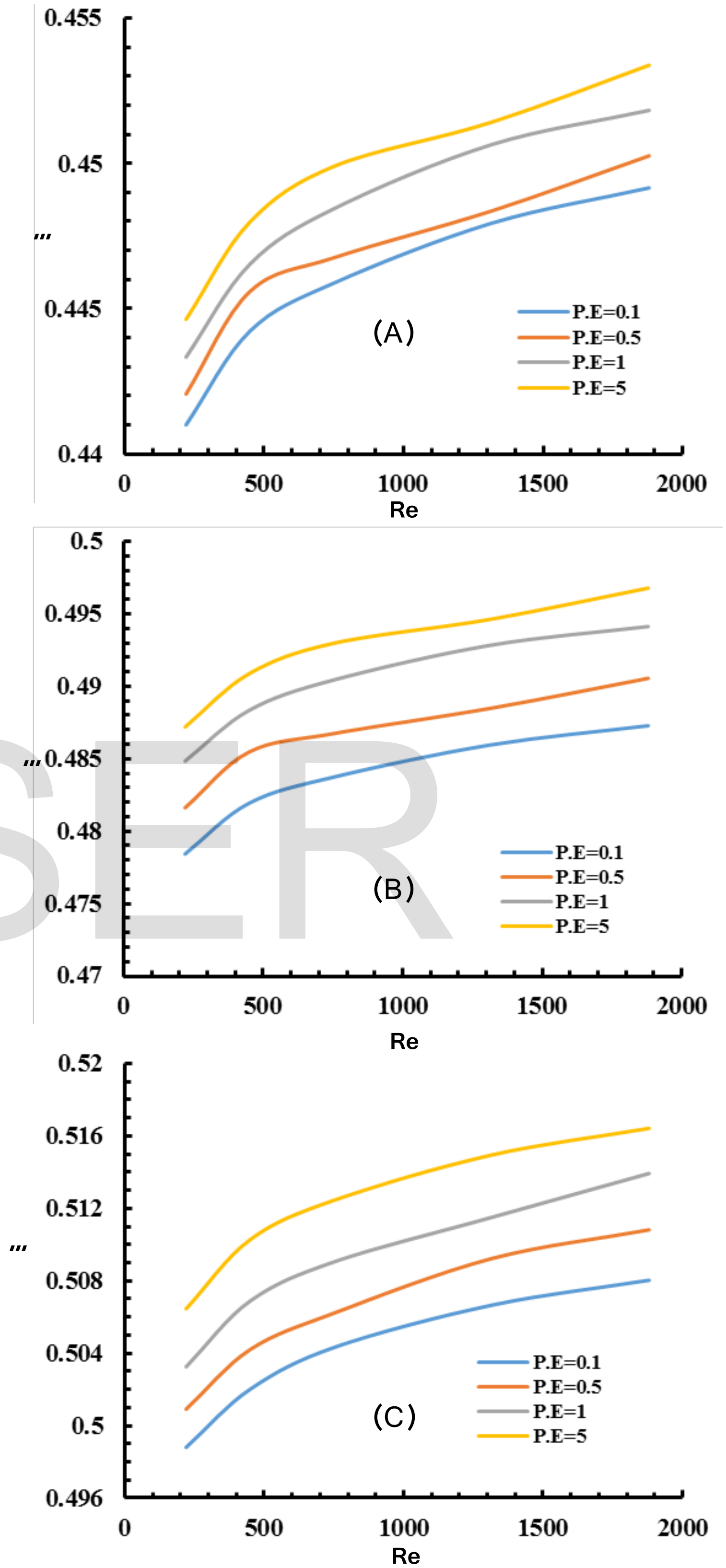

Fig.(7). Variation of stream function with (Re) for different values of P.E where (A) Pr=1.67 (B) Pr=4.67 (C) Pr=13.67

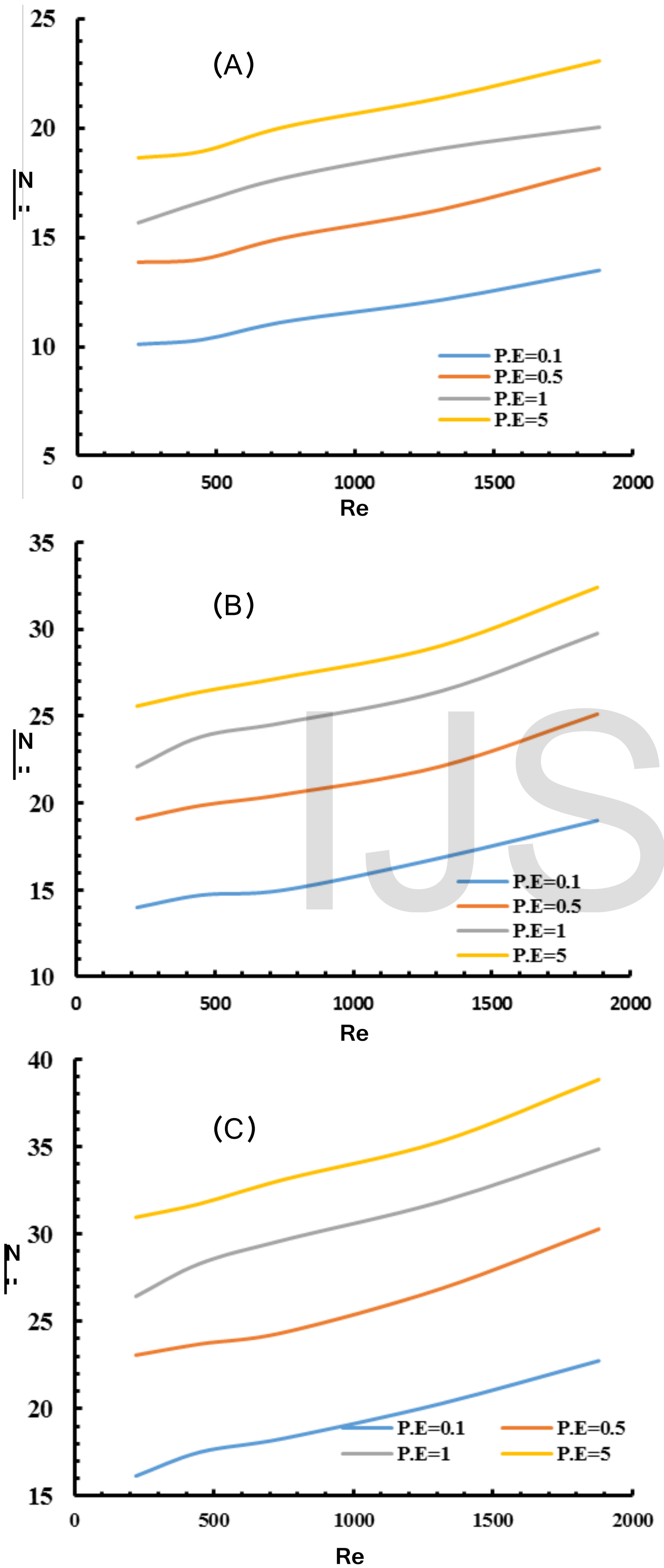

Fig.(8). Variation of Average Nusselt No. with (Re) for different value of P.E where (A) Pr=1.67 (B) Pr=4.67 (C) Pr=13.67

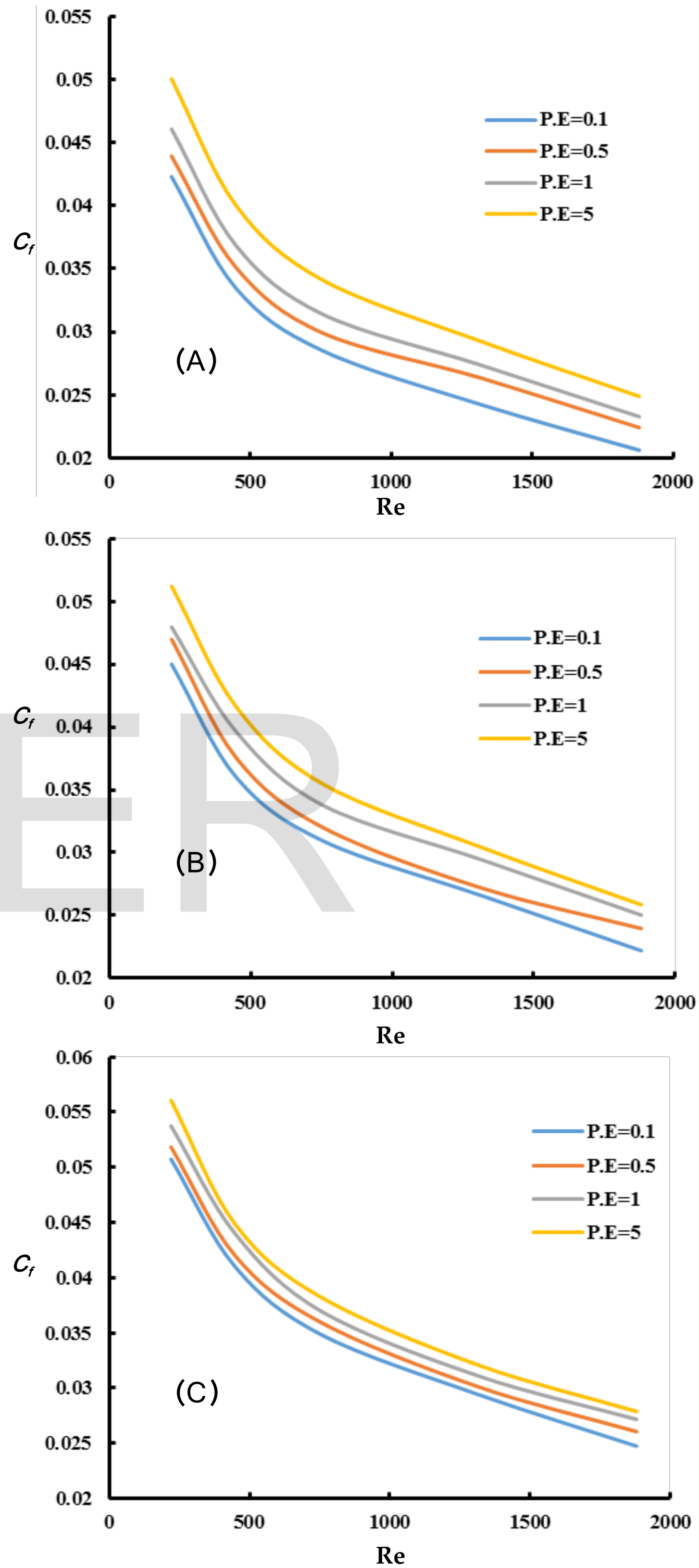

Fig.(9). Variation of Coeffiecient of friction with (Re) for different values of P.E and Pr=4.67

The effect of power law model (P.E) and prandtl number (Pr) on the coefficient of friction is represented in figure (9) for different Reynolds numbers. Usually, the coefficient of friction is given as the ratio of the total drop of pressure to the losses of Kinetic energy. The coefficient of friction increase slightly with the (P.E) in addition to the decrease in the flow rate and Re. When the flow rate is low, the coefficient of friction is related with pressure drop because small losses of kinetic energy. While the increasing in Reynolds number, the losses of kinetic energy become important, so the coefficient of friction will decrease.

6. Conclusion

The present numerical solutions for forced convection heat transfer of non- Newtonian fluid in a circular tube under constant heat flux was clearing up in this study. Its demonstrated that Nusselt number is a strong function of prandtl number, Reynolds number and power law model. The increase of (P.E) will lead to increase in heat transfer rate. Also, at the given Reynolds number, the increase in (Pr) has an efficient increasing of both local and Average Nusselt number. The effect of increasing of power law model and prandtl number will increase and enhance of stream function at given Reynolds number. However, at the same Reynolds number, increasing of prandtl number has a small effect on increase of coefficient of friction.

REFERENCES

1- Yogosh H.S. (2002). Numerical investigation of the Greatz problem for Newtonian and non-Newtonian flows in circular segment ducts. M.Sc. University of Bombay, India.

2- Chhabra R.P., Kanpur, Soares A. A. and Ferreira J. M(2004). Steady non–Newtonian flow past a circular cylinder: a numerical study. Springer, Acta micanica, Volume 172, Issue 1–2, pp 1–16.

3- Nagendra N., Subba Rao, Amanulla A., Reddy v., MSN, Beg, OA and Kadir.(2017). Numerical study of hydro-magnetic non-Newtonian nanofluid transport phenomena from a horizontal cylinder with thermal slip : aerospace nanomaterial enrobing simulation. Journal Of Nanofluids, Volume 7, Issue 1, pp. 115-128.

4- Soares A. A., Ferreira1 J. M. and Chhabra R. P. (2008). steady two dimensional non- Newtonian flow past an array of long circular cylinder up to Reynold's number 500: A numerical study. The Canadian Journal of Chemical Engineering, Volume 83, Issue 3, Version 19.

5- Muzychka Y. S. and Edge, J. (2008). Laminar Non-Newtonian Fluid Flow in Non-Circular Ducts and Micro-Channels. ASME J. Fluids Eng., 130, p.111-201.

6- Apurba Kumar Santra, Swarnendu Sen and Niladri Chakraborty. (2009). Study of heat transfer due to laminar flow of copper–water nanofluid through two isothermally heated parallel plates. Volume 48, Issue 2, p.p 391-400.

7- Ijam A. (1977). Finite element solution of incompressible viscous flow. Ph.D. thesis, Mechanical engineering department, Wales university.

8- Jannan W.S. (1988). Engineering heat transfer. S.I. Edition.

9- Coulson J.M. and Richardson J.S.(1971). Chemical Engineering. Bergamon, International Library, Volume 3.

10- Peterka A. and Richardson D. P. (1984). Effect of Sound on Local transport from a heated Cylinder. International heat-mass transfer. Volume 27, No.9, p.p1511-1523

11- Anderson A.D., Tannehill C.J. and Pletcher H.R. (1984). Computational fluid Mechanics and heat transfer.

12- Frank K. and MrakS. (1997). Principles of heat transfer. 5th Edition, PWS publishing company.